

## Atomic structure of the ectodomain from HIV-1 gp41

W. Welssenhorn\*†‡, A. Dessen\*‡, S. C. Harrison\*†‡, J. J. Skehel§ & D. C. Wiley\*†‡

\* Laboratory of Molecular Medicine and † Howard Hughes Medical Institute, The Children's Hospital, 320 Longwood Avenue, Boston, Massachusetts 02215, USA

‡ Department of Molecular and Cellular Biology, Howard Hughes Medical Institute, Harvard University, 7 Divinity Avenue, Cambridge, Massachusetts 02138, USA

§ National Institute of Medical Research, Mill Hill, The Ridgeway, London NW7 1AA, UK

‡ These authors contributed equally to this work

Fusion of viral and cellular membranes by the envelope glycoprotein gp120/gp41 effects entry of HIV-1 into the cell. The precursor, gp160, is cleaved post-translationally into gp120 and gp41 (refs 1, 2), which remain non-covalently associated. Binding to both CD4 and a co-receptor leads to the conformational changes in gp120/gp41 needed for membrane fusion<sup>3</sup>. We used X-ray crystallography to determine the structure of the protease-resistant part<sup>4,5</sup> of a gp41 ectodomain solubilized with a trimeric GCN4 coiled coil in place of the amino-terminal fusion peptide<sup>6</sup>. The core of the molecule is found to be an extended, triple-stranded  $\alpha$ -helical coiled coil with the amino terminus at its tip. A

carboxy-terminal  $\alpha$ -helix packs in the reverse direction against the outside of the coiled coil, placing the amino and carboxy termini near each other at one end of the long rod. These features, and the existence of a similar reversal of chain direction in the fusion pH-induced conformation of influenza virus HA2 (ref. 7) and in the transmembrane subunit of Moloney murine leukaemia virus<sup>8</sup> (Fig. 1a–d), suggest a common mechanism for initiating fusion.

A soluble crystalline GCN4/gp41 chimaera (Fig. 1) composed of the first 31 residues of a trimeric GCN4 isoleucine zipper<sup>9</sup>, the proposed zipper domain of gp41, residues 30–79 (refs 10, 11), and the C-terminal helical segment of gp41, residues 113–154 (refs 4, 5, 11), was produced by expressing the two segments in bacteria, refolding *in vitro*, and trimming with protease<sup>6</sup>. It lacks the 33 proteolytically sensitive residues 80–112, which contain a short disulphide loop and two oligosaccharide sites. It also lacks the 18 C-terminal residues of the gp41 ectodomain<sup>4–6</sup>. Electron microscopy indicates that the recombinant chimaera lacking these protease-sensitive regions has the same elongated, rod-like shape as an intact gp41 ectodomain expressed and secreted in insect cells<sup>12</sup>. The structure was determined by isomorphous replacement. The final model contains residues 1–77 and 117–154 and 15 solvent molecules.

The structure is a strikingly regular trimeric rod (Fig. 2a, b). There is a central  $\alpha$ -helical coiled coil (residues 1–77) 115 Å long and an antiparallel outer  $\alpha$ -helical layer (residues 117–154) 60 Å long. The  $\alpha$ -helices are packed together in the classical 'knobs into holes' arrangement<sup>13</sup>, but the outer layer packs differently onto the core from the way predicted by helical wheel sequence analysis and biochemical data<sup>4,5</sup>. Along the length of the central three-stranded coiled coil there are 15 layers of homotrimeric interactions in which successive 'a' and 'd' positions of the heptad repeats (A30L34IQ-LIQLTILIVLQ79; Fig. 1e) pack together on the molecular threefold symmetry axis. The C-terminal helices (117–154) run antiparallel from opposite position 65 of the core helices back to position 30 (Fig. 2b). Each C-terminal helix follows approximately the groove between two core helices. The connection of a core helix to a C-terminal helix is not present in our structure. The shortest path from the C terminus of one to the N terminus of the other links a core helix to its anticlockwise C-terminal neighbour, viewed from the 'fusion peptide' (Fig. 2a, b). This direction for the linker agrees with the direction of chain reversal seen in the influenza HA2 fusion pH structure and in the transmembrane (TM) subunit of Moloney murine leukaemia virus (MoMuLV) (Fig. 1a–c).

Because they run along a groove but lie at a larger radius, the outer-layer helices are tilted with respect to the core helices by approximately 15 degrees. Typical layers of packed side chains are shown in Fig. 2c, d. The relative tilt of core and outer-layer helices leads to a gradual drift in axial registration of the layers so that there is some irregularity near the 'bottom' of the bundle (Fig. 2 legend). A cluster of conserved tryptophan residues (W60, W117 and W120) dominate the helical packing in this region, and their bulk increases the interhelix spacing (Fig. 2c). Near the midpoint of the structure there is a cluster of conserved glutamine residues, and a network of hydrogen bonds links several glutamine and asparagine side chains near residue 40 in the core with a similar cluster near residue 142 in the outer layer (Fig. 2d). The Gln 41 side chains, at 'a' positions, face each other across the threefold axis. Several other hydrogen bonds and salt bridges seem to stabilize the observed structure. Most of these non-polar and polar interactions are from conserved or conservatively substituted residues in HIV-1, HIV-2 and simian immunodeficiency virus (SIV) (Fig. 1e).

The coiled-coil core extends beyond the outer helical layer at both ends (Fig. 2a, b). At its C-terminal end (residue 77, bottom in Fig. 2a), the overhang is five helical turns, or about 25 Å. This overhang would be linked to an outer-layer helix by 39 residues. The missing linker would contain a disulphide loop and two conserved glycosylation

sites. The outer-layer helices begin at residue 117. In complete gp41 the helices probably begin at approximately this point because there is a glycosylation site at the preceding heptad position (113) in the HX2B strain.

GCN4/gp41 from HIV-1, the fusion pH-induced conformation of influenza virus HA2 (ref. 7), and the TM fragment of the MoMuLV<sup>8</sup> share three features of overall molecular organization (Fig. 1a-c). First, the N-terminal fusion peptide is at the tip of a triple-stranded,  $\alpha$ -helical coiled coil. In the case of influenza haemagglutinin, it is known that the fusion pH-induced conformational change uncovers the fusion peptide and causes it to move more than 100 Å from the centre of the molecule to one end, as the result of extension of the coiled-coil core by 36 residues<sup>7,14,15</sup> (Fig. 1c, d). Second, the polypeptide chain reverses direction at the other end of the coiled coil and proceeds back towards the N-terminal tip. The turn occurs at the same place in HIV-1 gp41 and MoMuLV subunit, residue 78, and is followed by a glycine-rich stretch of eight residues and a disulphide loop of seven (HIV-1) or eight (MoMuLV)

residues (Fig. 1b), suggesting further structural similarities between gp41 and the transmembrane components of other retroviruses. Third, the C-terminal link leading to the transmembrane anchor is probably flexible. It is exposed to proteolysis in the retroviral and influenza virus proteins<sup>4-6,8,16</sup>, and it is structurally disordered in the fusion pH-induced conformation of HA2 (ref. 7).

The flexibly linked transmembrane anchors and the fusion peptides may be constrained to the same end of the coiled coil by the shared features just outlined. The C terminus of the proteolytically resistant core of GCN4/gp41, residue 154, is only 18 residues from the transmembrane anchor, yet it lies nearly at the N-terminal end of the helical rod, over 75 Å from the 'bottom' of the coiled coil (Fig. 2a). In the influenza virus HA2 structure, the last observed residue is 23 residues from the transmembrane anchor, and it also lies close to the N-terminal end of the helical rod, approximately 70 Å from the 'bottom' of the coiled coil (Fig. 1c). The last residue in the crystalline fragment (the central 40%) of the MoMuLV TM subunit (46-97) is 37 residues from the transmembrane anchor and

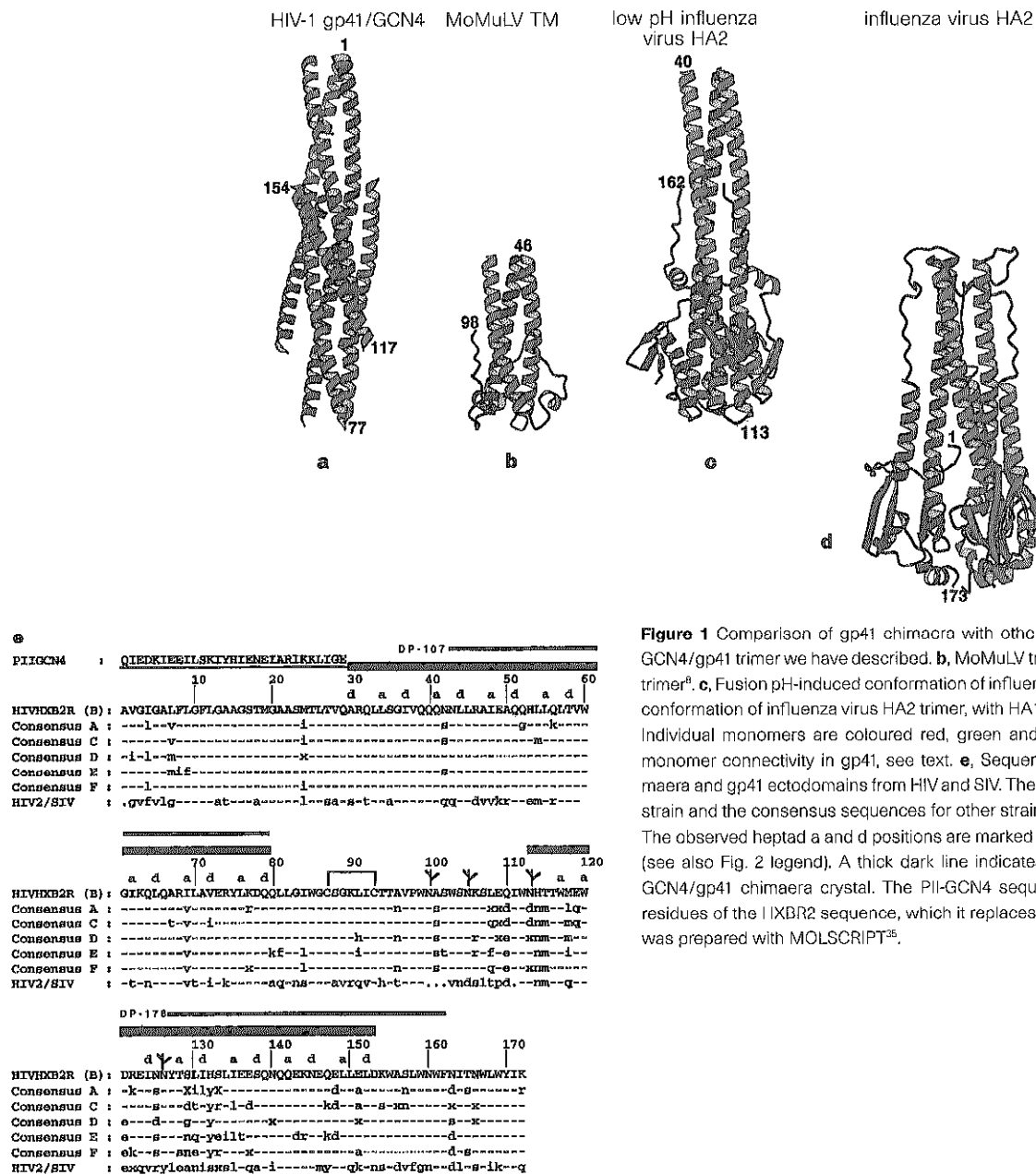


**Figure 1** Comparison of gp41 chimaera with other viral glycoproteins. **a**, The GCN4/gp41 trimer we have described. **b**, MoMuLV transmembrane (TM) subunit trimer<sup>8</sup>. **c**, Fusion pH-induced conformation of influenza virus HA2 (ref. 7). **d**, Initial conformation of influenza virus HA2 trimer, with HA1 domains omitted for clarity. Individual monomers are coloured red, green and purple. For assignment of monomer connectivity in gp41, see text. **e**, Sequences of the GCN4/gp41 chimaera and gp41 ectodomains from HIV and SIV. The sequence of the HIV HXBR2 strain and the consensus sequences for other strain classes have been listed<sup>31</sup>. The observed heptad a and d positions are marked above the HXBR2 sequence (see also Fig. 2 legend). A thick dark line indicates the portion of gp41 in the GCN4/gp41 chimaera crystal. The PII-GCN4 sequence<sup>9</sup> is above the first 29 residues of the HXBR2 sequence, which it replaces in the chimaera. This figure was prepared with MOLSCRIPT<sup>36</sup>.

lies roughly midway along the coiled coil formed by residues 46–78 (Fig. 1b). Circular dichroism indicates that part of the C-terminal segment omitted from the crystallized fragment of the MoMuLV TM subunit is  $\alpha$ -helical<sup>8</sup>. Taken together these observations suggest that once the outer layer around the central coiled coil has zipped into place, the transmembrane anchors and fusion peptides will be at the same end of the rod-shaped molecules. Electron microscopy and antibody labelling of membrane-associated HA2 provide direct evidence for this suggestion<sup>17</sup>.

Binding of the HIV envelope glycoprotein to its receptors results in increased exposure of gp41 and ultimately to the dissociation of gp120 (refs 18–20). Thus we expect gp41 produced in the absence of gp120 to adopt the conformation of its fusion-active state, just as influenza virus HA2 produced in bacteria in the absence of HA1 adopts its fusion pH-induced conformation<sup>7,21</sup>. The long coiled-coil

structures in recombinant gp41, the MoMuLV TM subunit and HA2 expressed in the absence of their receptor-binding subunits<sup>5,8,12,21</sup>, and in viral HA2 in the fusion pH-induced conformation<sup>16</sup>, are all extremely thermostable. These observations are consistent with the expectation that, once triggered by interaction with the cell or transfer into endosomes, some viral fusion proteins switch irreversibly during fusion from a metastable to a stable conformation.

Evidence that infectivity requires a conformational change in gp41, rather than merely 'uncapping' by dissociation of gp120, comes from the properties of site-directed point mutations in the coiled coil and from the mechanism of inhibition of HIV-1 infectivity by peptides derived from gp41 (refs 22–24). Mutations at Ile 62, an 'a' heptad position in the coiled coil (Figs 1e, 2c), inhibit both membrane fusion and viral infectivity without preventing formation

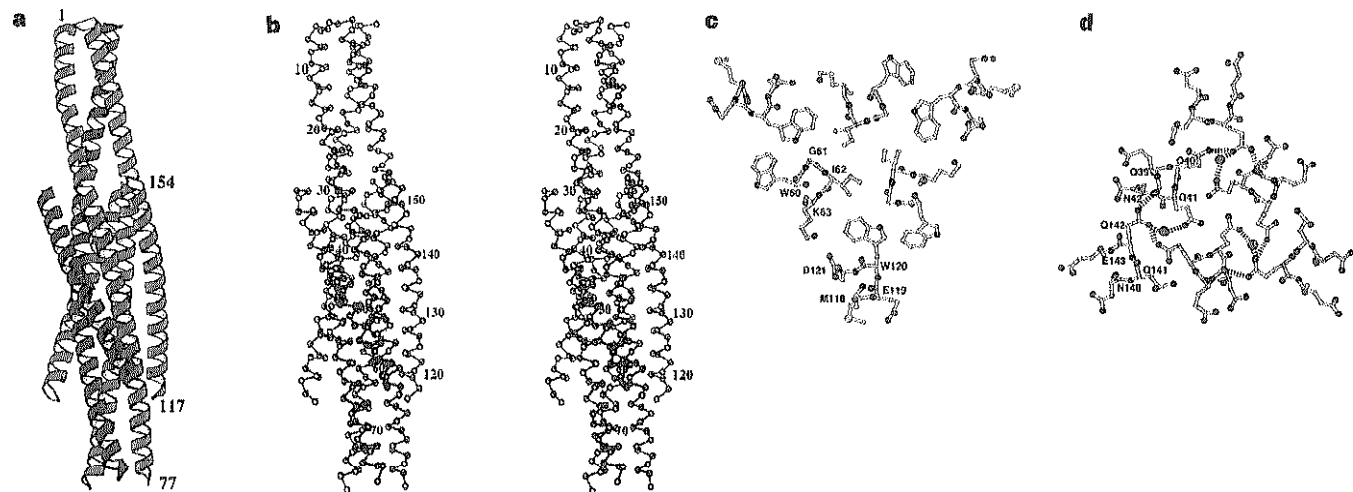


**Figure 2** GCN4/gp41 chimaera structure. **a**, Ribbon drawing of trimeric GCN4/gp41. **b**,  $\alpha$  stereo drawing of trimeric GCN4/gp41, labelled every 10 residues. **c**, Helix packing in gp41, seen in cross-section at two levels in the structure. Homotrimeric packing of I62, intra-chain packing of W120 against I62 of the same molecule, and W120 against an adjacent core helix in the oligomer. (Labels are all on one monomer.) **d**, Packing in the glutamine (Q)-rich layer around residues 41 and 142 in the core and outer layers, respectively. Hydrogen bonds are shown in green as broken lines. A bound solvent molecule is shown as an isolated red circle, linked by hydrogen bonds to Q141 and Q142. Q141 in the outer layer (and

Y127, L134, E148) makes pseudo-twofold contacts with one of the core helices, not pseudo-threefold contacts as predicted<sup>4,b</sup>. Successive a and d positions of each outer layer helix (W117 W120 I124 T128 I131 I135 SQNLL152; Figs 1e, 2b) form 11 layers of pseudo-threefold contacts with the two adjacent core helices. Alternate aag and dde heptad layers form this interface except at the first layer (W117), which is dae; there is also one extra residue between 'a' 120 and 'd' 124. (The designations aag and dde refer to a core helix, a C-terminal helix, and a second core helix, respectively, in anticlockwise order as viewed from the GCN4 end.) This figure was prepared using MOLSCRIPT<sup>25</sup>.

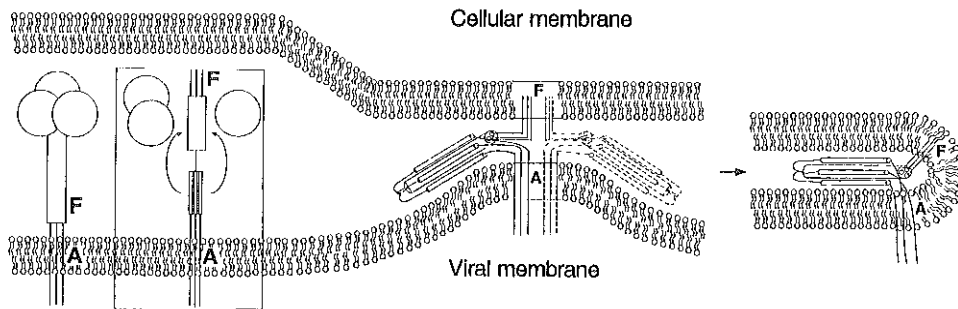


**Figure 3** A model for the interaction with membranes of gp41 and other viral fusion subunits, during membrane fusion. Left, before fusion, viral glycoproteins project their receptor-binding domains (spheres) towards the cellular membrane. Brackets, a conformational change extends the N-terminal fusion peptide (F) towards the cellular membrane. Centre, after the outer layer of the fusion has assembled, the N-terminal fusion peptides (F) and the C-terminal transmembrane anchors (A) lie near each other at a site of close

apposition of the prefusion membranes. Flexible links between the central rod and the F and A segments allow variable orientations of the rod with respect to the two membranes. A second trimer, shown in dotted lines, indicates how such trimers might aggregate at their hydrophobic ends at initial sites of fusion. Right, after membrane fusion, both the fusion peptides (F) and transmembrane anchors (A) are shown in the same membrane, as suggested previously<sup>7,17,26</sup>.

**Table 1 Statistics for data collection, phase determination and refinement**

| Crystal                                               | Native   | OsO <sub>4</sub> | K <sub>2</sub> PtBr <sub>4</sub> | HgI <sub>4</sub> |                                   |
|-------------------------------------------------------|----------|------------------|----------------------------------|------------------|-----------------------------------|
| Resolution limit (Å)                                  | 2.6      | 2.6              | 3.0                              | 3.3              |                                   |
| R <sub>sym</sub> (%) <sup>*</sup>                     | 71       | 9.7              | 9.7                              | 9.8              |                                   |
| Completeness                                          | 90.5     | 87.9             | 86.1                             | 91.5             |                                   |
| R <sub>deriv</sub> (%) <sup>†</sup>                   |          | 14.0             | 15.7                             | 27.0             |                                   |
| Sites                                                 |          | 2                | 1                                | 1                |                                   |
| Phasing power (acentric/centric) <sup>‡</sup>         |          | 1.58/1.24        | 1.16/0.78                        | 1.22/1.14        |                                   |
| R <sub>critic</sub> (% acentric/centric) <sup>§</sup> |          | 73/59            | 84/73                            | 82/74            |                                   |
| Refinement <sup>  </sup>                              |          |                  |                                  |                  |                                   |
| Resolution                                            | 25–2.6 Å |                  |                                  |                  |                                   |
| R <sub>free</sub> (%)                                 | 27.7     |                  |                                  |                  |                                   |
| R <sub>cryst</sub> (%)                                | 24.4     |                  |                                  |                  |                                   |
|                                                       |          | R.m.s.d.         |                                  |                  |                                   |
|                                                       | Res. No. | Average B-factor | Bonds (Å)                        | Angles (°)       | B-factors (Å <sup>2</sup> bonded) |
| Protein                                               | 115      | 53.1             | 0.010                            | 1.20             | 4.5                               |
| Water                                                 | 15       | 54.2             |                                  |                  |                                   |

<sup>\*</sup>R<sub>sym</sub> = Σ || (I) / Σ I, where I is the observed intensity, and (I) is the average intensity of multiple observations of symmetry-related reflections.

<sup>†</sup>R<sub>deriv</sub> = Σ || F<sub>PH</sub> | - | F<sub>P</sub> || / Σ | F<sub>P</sub> |, where | F<sub>P</sub> | is the protein structure factor amplitude and | F<sub>PH</sub> | is the heavy-atom derivative structure factor amplitude.

<sup>‡</sup>Phasing power = r.m.s. (| F<sub>PH</sub> | / E), where | F<sub>PH</sub> | is the heavy-atom structure factor amplitude, and E is the residual lack of closure error.

<sup>§</sup>R<sub>critic</sub> = Σ | E | / (Σ | F<sub>PH</sub> | - | F<sub>P</sub> |).

<sup>||</sup>R = Σ || F<sub>O</sub> | - | F<sub>C</sub> || / Σ | F<sub>O</sub> |, where R<sub>free</sub> is calculated for a randomly chosen 10% of reflections, and R<sub>cryst</sub> is calculated for the remaining 90% of reflections (F > 2.0) used for structure refinement.

of gp120/gp41 oligomers<sup>25</sup>. Ile 62 makes a homotrimeric contact at the centre of the coiled coil and interacts with Trp 120 of the outer helix, in the cluster of conserved tryptophans (Fig. 2c). Polar mutations at 62 would destabilize both the coiled coil itself and its association with the outer helix, potentially exerting a greater effect on the fusion state of gp41 than on the oligomerization of gp120/gp41 (refs 23, 25), thus inhibiting the conformational transition.

Peptides having the sequence of residues 42–72 and 127–162 from gp41 (Fig. 1e) have anti-HIV activity and block membrane fusion<sup>22–24</sup>. In GCN4/gp41 these regions interact directly: 42–72 is part of the coiled-coil sequence against which the outer helix segment 127–162 packs. We would not expect these peptides to interact with the structure of gp41 seen here, which is too stable to be disrupted by their binding. Indeed, our structure supports the proposal that these peptides exert their effects by interacting with gp41 during the conformational change to the fusion-active conformation<sup>24</sup>. Only before or during that conformational change would we expect the targets for the peptides to be available. Peptide 42–72 could target the incipient outer-layer helix and peptide 127–162 the surface of the awaiting coiled coil. This interpretation is consistent with the lack of inhibitory action observed with a preassembled complex containing both the coiled coil and the outer-layer helices<sup>5</sup>. Whatever the actual inhibitory mechanism of these peptides, it should indeed be possible to design or discover small-molecule drugs that reduce the infectivity of HIV, influenza or other viruses by interfering with chain reversal, as suggested here.

By analogy with the changes in influenza haemagglutinin structure induced at fusion pH, the conformational change in gp41 required for activation of membrane fusion by association of the envelope glycoprotein with its receptor might also include formation of the complete coiled coil by extension at the N terminus. For example, the glutamine-rich segments near residues 41 and 51 described earlier (Fig. 1e) might not be α-helical in native gp120/gp41. Like the 'B-loop' in influenza HA2, which undergoes a loop-to-helix transition at the fusion pH (refs 7, 15), gp41 is particularly rich in polar and charged side chains between residues 39 and 53.

The observation that conformational changes in a membrane fusion protein uncover its fusion peptide has led to the expectation that the exposed hydrophobic peptide would initiate fusion by inserting into a membrane, probably the cellular membrane<sup>14,26</sup>. The

observation that, during its fusion pH-induced conformational change, influenza HA2 folds back and assembles an outer layer around a central coiled coil<sup>7</sup> has led to the notion that in the postfusion state there would be an inverted molecule with both ends in the same membrane<sup>7,17</sup>. Flexible linkages between the central rod-like segment and the membrane insertions at either end would allow the molecule to bend as the outer layer forms, thereby bringing the apposed membranes more closely together than the length of the rod itself<sup>6,7,26</sup>. The structure of GCN4/gp41 suggests, more strikingly than previous structures, that the fusion peptides and transmembrane anchors of the fusion glycoproteins are likely to be juxtaposed at one end of the coiled coil, once the outer layer of helices has assembled onto the core. This arrangement would promote a close apposition of viral and cellular membranes, as suggested in Fig. 3. The transmembrane anchors and fusion segments on the envelope protein of tick-borne encephalitis and other flaviviruses may also be juxtaposed near one end of the extended molecule, which even in the native virion lies parallel to the viral membrane<sup>27</sup>.

The presence of the hydrophobic fusion peptide and transmembrane anchors in two bilayers in direct apposition may be central to overcoming the 'hydration force'<sup>28</sup> that is a barrier to membrane fusion. The nonlinear dependence on fusion-protein surface density of a kinetic lag in the reaction suggest that several trimers may assemble to create this pore<sup>29</sup>. It is possible that long, rod-shaped molecules may cluster at their hydrophobic tips (Fig. 3), forming asters with centres that could be the points of initial membrane fusion (see, for example, ref. 30). Since this paper was submitted, the structure of a smaller fragment of gp41 has been reported<sup>31</sup>. □

**Methods**

**Diffraction data.** The GCN4/gp41 chimaera pII41NC(113–154) was prepared as described<sup>6</sup>. Crystals were grown in hanging drops by combining 1 μl protein solution (15–20 mg ml<sup>-1</sup> in 20 mM HEPES, pH 8.3, 75 mM NaCl) with 1 μl of reservoir solution (100 mM HEPES, pH 8.0, 1.1 M ammonium sulphate, 12% ethylene glycol). They belong to space group R32, a = 52.37 Å, b = 52.37 Å, c = 414.52 Å, one monomer per asymmetric unit. Diffraction data were recorded at room temperature, using a Mar image plate detector and an Elliot GX-13 rotating anode source with mirror optics, and processed using the programs DENZO and SCALEPACK (HKL Research).

**Structure determination.** The structure was determined by multiple isomorphous replacement (MIR). For derivatization, crystals were soaked in 0.5 mM K<sub>2</sub>OsO<sub>4</sub> for 48 h, in 200 mM K<sub>2</sub>PtBr<sub>4</sub> for 7 days, and in 1 mM K<sub>2</sub>HgI<sub>4</sub>

for 60 h at room temperature. Native and derivative data were scaled using CCP4 programs<sup>32</sup>. One Os site was located in a difference Patterson map; an additional Os site, one Pt site, and one Hg site were found in difference Fourier maps. Heavy-atom positions were refined and phases were calculated using MLPHARE<sup>32</sup>. Both an SIR map calculated solely with Os phase information (including anomalous scattering) and an MIR map, calculated with all derivatives, were improved by density modification using the program DM<sup>32</sup>. These maps allowed assignment of 92 of the 121 residues of the GCN4/gp41 molecule in the density, using the program O (DATAONO AB). Combined model and MIR phases led to an improved MIR map, which then revealed all except 6 of the remaining residues. Cycles of rebuilding, positional refinement and thermal-parameter refinement<sup>33</sup> were used to improve the model, as judged by the free *R*-factor<sup>33</sup>. The model was submitted to simulated annealing from 3,000K after *R*<sub>free</sub> had dropped below 34%, after which further rebuilding and refinement yielded a model with *R*<sub>free</sub> = 27.7% and *R*<sub>cryst</sub> = 24.4% to 2.6 Å (all data); see Table 1. The refined model includes residues 1–77 in the long helix and 117–154 in the short helix, as well as 15 water molecules. The four N-terminal amino acids of the short helix, 113–116, did not have identifiable density in difference maps; they may be poorly ordered. Despite high thermal parameters in the GCN4 region, the chain is clear throughout the entire model.

Received 16 April; accepted 1 May 1997.

- Allan, J. S. *et al.* Major glycoprotein antigens that induce antibodies in AIDS patients are encoded by HTLV-III. *Science* **228**, 1091–1094 (1985).
- Veronese, F. D. *et al.* Characterization of gp41 as the transmembrane protein coded by the HTLV-III/LAV envelope gene. *Science* **229**, 1402–1405 (1985).
- D'Souza, M. P. & Harden, V. A. Chemokines and HIV-1 second receptors: confluence of two fields generates optimism in AIDS research. *Nat. Med.* **2**, 1293–1300 (1996).
- Blacklow, S. C., Lu, M. & Kim, P. S. A trimeric subdomain of the simian immunodeficiency virus envelope glycoprotein. *Biochemistry* **34**, 14955–14962 (1995).
- Lu, M., Blacklow, S. C. & Kim, P. S. A trimeric structural domain of the HIV-1 transmembrane glycoprotein. *Nature Struct. Biol.* **2**, 1075–1082 (1995).
- Weissenhorn, W. *et al.* Assembly of a rod-shaped chimera of a trimeric GCN4 zipper and the HIV-1 Gp41 ectodomain expressed in *E. coli*. *Proc. Natl Acad. Sci. USA* (in the press).
- Bullough, P. A., Hughson, F. M., Skehel, J. J. & Wiley, D. C. Structure of influenza haemagglutinin at the pH of membrane fusion. *Nature* **371**, 37–43 (1994).
- Fass, D., Harrison, S. C. & Kim, P. S. Retrovirus envelope domain at 1.7 Å resolution. *Nature Struct. Biol.* **3**, 465–469 (1996).
- Harbury, P. B., Kim, P. S. & Alber, T. Crystal structure of an isoleucine-zipper trimer. *Nature* **371**, 80–83 (1994).
- Chambers, P., Pringle, C. R. & Easton, A. J. Heptad repeat sequences are located adjacent to hydrophobic regions in several types of virus fusion glycoproteins. *J. Gen. Virol.* **71**, 3075–3080 (1980).
- Gallagher, W. R., Ball, J. M., Garry, R. F., Griffin, M. C. & Montelaro, R. C. A general model for the transmembrane proteins of HIV and other retroviruses. *AIDS Res. Hum. Retroviruses* **5**, 431–440 (1989).
- Weissenhorn, W. *et al.* The ectodomain of HIV-1 env subunit gp41 forms a soluble, alpha-helical, rod-like oligomer in the absence of gp120 and the N-terminal fusion peptide. *EMBO J.* **15**, 1507–1514 (1996).
- Crick, F. H. C. The Fourier transform of a coiled-coil. *Acta Crystallogr.* **6**, 685 (1953).

- Skehel, J. J. *et al.* Changes in the conformation of influenza virus haemagglutinin at the pH optimum of virus-mediated membrane fusion. *Proc. Natl Acad. Sci. USA* **79**, 968–972 (1982).
- Carr, C. M. & Kim, P. S. A spring-loaded mechanism for the conformational change of influenza haemagglutinin. *Cell* **73**, 823–832 (1993).
- Ruigrok, R. W. *et al.* Studies on the structure of the influenza virus haemagglutinin at the pH of membrane fusion. *J. Gen. Virol.* **69**, 2785–2795 (1988).
- Wharton, S. A. *et al.* Electron microscopy of antibody complexes of influenza virus haemagglutinin in the fusion pH conformation. *EMBO J.* **14**, 240–246 (1995).
- Moore, J. P., McKeating, J. A., Weiss, R. A. & Sattentau, Q. J. Dissociation of gp120 from HIV-1 virions induced by soluble CD4. *Science* **250**, 1139–1142 (1996).
- Hart, T. K. *et al.* binding of soluble CD4 proteins to human immunodeficiency virus type 1 and infected cells induces release of envelope glycoprotein gp120. *Proc. Natl Acad. Sci. USA* **88**, 2189–2193 (1991).
- Kirsh, R. *et al.* Morphometric analysis of recombinant soluble CD4-mediated release of the envelope glycoprotein gp120 from HIV-1. *AIDS Res. Hum. Retroviruses* **6**, 1209–1212 (1990).
- Chen, J. *et al.* A soluble domain of the membrane-anchoring chain of influenza virus haemagglutinin (HA2) folds in *Escherichia coli* into the low-pH-induced conformation. *Proc. Natl Acad. Sci. USA* **92**, 12205–12209 (1995).
- Wild, C. T., Oas, T., McDanal, C. B., Bolognesi, D. & Matthews, T. A synthetic inhibitor of human immunodeficiency virus replication: Correlation between solution structure and viral inhibition. *Proc. Natl Acad. Sci. USA* **89**, 10537–10541 (1992).
- Wilfl, C. T., Shugart, D. C., Greenwell, T. K., McDanal, C. B. & Matthews, T. J. Peptides corresponding to a predictive alpha-helical domain of human immunodeficiency virus type 1 and gp41 are potent inhibitors of virus infection. *Proc. Natl Acad. Sci. USA* **91**, 9770–9774 (1994).
- Chen, C. H., Matthews, T. J., McDanal, C. B., Bolognesi, D. P. & Greenberg, M. L. A molecular clasp in the human immunodeficiency virus (HIV) type 1 TM protein determines the anti-HIV activity of gp41 derivatives: implication for viral fusion. *J. Virol.* **69**, 3771–3777 (1995).
- Dubay, J. W., Roberts, S. J., Brody, B. & Hunter, E. Mutations in the leucine zipper of the human immunodeficiency virus type 1 transmembrane glycoprotein affect fusion and infectivity. *J. Virol.* **66**, 4748–4756 (1992).
- Skehel, J. J. *et al.* Membrane Fusion by Influenza Hemagglutinin. *Cold Spring Harb. Symp. Quant. Biol.* **60**, 573–580 (1996).
- Rey, F. A., Heinz, F. X., Mandl, C., Kunz, C. & Harrison, S. C. The envelope glycoprotein from tick-borne encephalitis virus at 2 Å resolution. *Nature* **375**, 291–298 (1995).
- Leikin, S., Parsegian, V. A., Rau, D. C. & Rand, R. P. Hydration forces. *Annu. Rev. Phys. Chem.* **44**, 369–395 (1993).
- Danieli, T., Pelletier, S. L., Henis, Y. I. & White, J. M. Membrane fusion mediated by the influenza virus haemagglutinin requires the concerted action of at least three haemagglutinin trimers. *J. Cell Biol.* **133**, 559–569 (1996).
- Kanaseki, T., Kawasaki, K., Murata, M., Ikeuchi, Y. & Ohnishi, S.-I. Structural features of membrane fusion between influenza virus and liposome as revealed by quick-freezing electron microscopy. *J. Cell Biol.* (in the press).
- Chau, D. C., Fass, D., Berger, J. M. & Kim, P. S. Core structure of gp41 from the HIV envelope glycoprotein. *Cell* **89**, 263–273 (1997).
- CCP4 The CCP4 Suite: Programs for Protein Crystallography. *Acta Crystallogr. D* **50**, 760–776 (1994).
- Brlinger, A. T. *X-PLOR (Version 3.1) Manual* (Yale University, New Haven, CT, 1992).
- Myers, G. *et al.* in *Theoretical Biology and Biophysics Group, Los Alamos* (National Library, Los Alamos, NM, 1995).
- Kratulis, P. MOLSCRIP: a program to produce both detailed and schematic plots of protein structures. *J. Appl. Crystallogr.* **24**, 924–950 (1991).

**Acknowledgements.** We thank M. Pietras for technical assistance, and present and former members of the Harrison and Wiley groups, including M. Lawrence, R. Nolte, B. Temple, K. Smith, A. Musacchio, W. Xu, M. Eck, P. Rosenthal, R. Brown and S. Ray, for advice. The research was supported by grants from the NIH, the Howard Hughes Medical Institute (HHMI), and the MRC. S.C.H. and D.C.W. are investigators in the HHMI, and W.W. is an HHMI associate.

Correspondence and requests for materials should be addressed to D.C.W. (e-mail: wiley@xta10.harvard.edu). Coordinates will be deposited in the Brookhaven Protein Data Bank and are available pre-release at dessen@xta16.ch.harvard.edu.



